

KEPLERIAN ELEMENTS EVOLUTION IN ORBITAL MANEUVERS THROUGH SUPERPOSITION AND CORRELATED THRUST VECTOR DEVIATIONS

Antônio Delson C. de Jesus

Departamento de Física - Universidade Estadual de Feira de Santana
Km 03, BR 116, Campus Universitário, 44.031-460 – Feira de Santana – BA
adj@uefs.br

Fredson Braz Matos dos Santos

Departamento de Física - Universidade Estadual de Feira de Santana
Km 03, BR 116, Campus Universitário, 44.031-460 – Feira de Santana – BA
brazfr@uol.com.br

***Abstract.** We analyzed the effects of the correlation and superposition deviations thrust vector through the keplerian elements evolution in orbital maneuvers. We found cause vs. effect nonlinear relations for these dynamic and the limited power propulsion curve of the space vehicle.*

***Keywords.** orbital, maneuvers, thrust, superposition and correlation, deviation*

1. Introduction

The analysis of the keplerian elements evolution in orbital maneuvers under non-natural and natural uncertainties provides many important information for the spatial missions. The Earth natural environment introduces several dissipation effects in the orbital and attitude motion of space vehicles. These effects produce loss of energy and optimality in the vehicles dynamic. The satellite motion is deviated out of nominal trajectory and periodic correction maneuvers are required. Many natural effects can be observed in these nonlinear dynamics, due to many perturbations forces and torques: albedo, aerodynamic drag, atmospheric density, EUV radiation, solar and geomagnetic activity, Earth oblateness, gravity gradient, etc. These perturbations cause difficult to the knowledge of the instantaneous locations of orbiting satellite and their orbit predictions. Many critical control operations need are realized to collision avoidance, to satellite re-entry, satellite photo-reconnaissance, maintain certain formation of several satellites operating jointly, etc. The keplerian orbital elements are affected and the nominal trajectories do not reached, due the difficulty to model any these forces and torques. For example, atmospheric drag is the dominant and the most difficult force to determine and predict, in the orbit propagation model of low Earth orbiting satellites. Many authors studied all these natural effects in the satellites motion, through the different approach, interests of the missions or necessity and aspects of the motion. Jesus et al (2002) presented survey on the perturbations orbital problems. In this paper were considered many results with forces (non-rotational and non-sphericity atmosphere, solar radiation pressure, infrared, etc.) influences over the keplerian orbital elements of the maneuvers for an artificial satellite. Most the problems found by authors is in the model these forces and torques to found analytical solution of the nonlinear dynamic associated to the vehicles motion. The mutual coupling effects between the orbital and rotational motion was studied by many authors, see, e.g, Maciejewski (1995). These effects were observed in motion of extended bodies, e.g., a large artificial satellite, but the analytical description of this interaction is very complicated.

In this paper we call non-natural perturbations those produced on propulsion systems (during the thrusters burns) and on the engineering operations (manufacturing, kind of thrust operations, etc.). These perturbations too generate effects over the orbital elements of the satellite maneuvers. Porcelli and Vogel (1980) studied the orbit insertion deviations propagation in two-impulsive noncoplanar orbital transfers through the final keplerian elements and velocities components. Adams and Melton (1986) developed algorithm to calculate the propagation of guidance and navigation deviations along a impulsive trajectory involving finite-duration perigee burns in the semi-major axis, in the position and velocity initials, flight-path angle, and burn-on ignition time. Others authors used the propulsion system as control system to reach many purposes. See e.g., Kluever (1997), Javorsek II and Longuski (1999), Vassar and Sherwood (1985), Ulybyshev (1998), etc. Rodrigues (1991) and Santos-Paulo (1998) used one deterministic analysis of thrust errors effects to the impulsive assumption for the non-punctual satellite. Jesus (1999) developed one extensive numerical and analytical study about orbital transfer under thrust errors, gaussian and uniform distribution probabilistic errors. He found the numerical and analytical non-linear (near parabolic) relation between the cause (direction errors) and effect (keplerian elements errors), using the Monte-Carlo analysis for the numerical part. His analysis extended until the second moment of the uncertainties inside the keplerian elements. For the semi-major axis deviation the standard deviation has one linear relation for the usual cause errors. In this paper we present the results of the direction misalignments effects through the keplerian elements for the superposition and correlation thrust deviations. We developed one Monte-Carlo exact numerical analysis and found the cause/effect relation between the final keplerian elements and the pitch and yaw direction angle deviations to optimal continuous and non-coplanar transfers maneuvers. These angles are the control variables and provides the optimal (fuel consumption minimum) direction to thruster burn.

2. Mathematical Formulation and Coordinate Systems

The orbital transfers problem studied can be formulated in the following way:

- 1) Minimize the performance index: $J = m(t_0) - m(t_f)$;
- 2) With respect to $\alpha : [t_0, t_f] \rightarrow \mathbb{R}$ (pitch angle) and $\beta : [t_0, t_f] \rightarrow \mathbb{R}$ (yaw angle) with $\alpha, \beta \in C^{-1}$ em $[t_0, t_f]$;
- 3) Subject to the dynamics in inertial coordinates X_i, Y_i, Z_i of Figure (1): $\forall t \in [t_0, t_f]$,

$$m(t) \cdot \frac{d^2 X}{dt^2} = \frac{-\mu \cdot m(t) \cdot X}{R^3} + F_X \quad (1)$$

$$m(t) \cdot \frac{d^2 Y}{dt^2} = \frac{-\mu m(t) \cdot Y}{R^3} + F_Y \quad (2)$$

$$m(t) \cdot \frac{d^2 Z}{dt^2} = \frac{-\mu \cdot m(t) \cdot Z}{R^3} + F_Z \quad (3)$$

$$F_X = F[\cos \beta \cdot \sin \alpha \cdot (\cos \Omega \cdot \cos \theta - \cos I \cdot \sin \Omega \cdot \sin \theta) + \sin \beta \cdot \sin \Omega \cdot \sin I - \cos \beta \cdot \cos \alpha \cdot (\cos \Omega \cdot \sin \theta + \cos I \cdot \sin \Omega \cdot \cos \theta)] \quad (4)$$

$$F_Y = F[\cos \beta \cdot \sin \alpha \cdot (\sin \Omega \cdot \cos \theta + \cos I \cdot \cos \Omega \cdot \sin \theta) - \sin \beta \cdot \cos \Omega \cdot \sin I - \cos \beta \cdot \cos \alpha \cdot (\sin \Omega \cdot \sin \theta - \cos \Omega \cdot \cos I \cdot \cos \theta)] \quad (5)$$

$$F_Z = F(\cos \beta \cdot \sin \alpha \cdot \sin I \cdot \sin \theta + \cos \beta \cdot \cos \alpha \cdot \sin I \cdot \cos \theta + \sin \beta \cdot \cos I) \quad (6)$$

$$m(t) = m(t_0) + \dot{m} \cdot (t - t_0), \quad (7)$$

$$F \cong |\dot{m}| \cdot c \quad (8)$$

with $\dot{m} < 0$

Or in orbital coordinates (radial R, transversal T, and binormal N) of Figure (2):

$$m(t) \cdot a_R(t) = F \cdot \cos \beta(t) \cdot \sin \alpha(t) - \frac{\mu \cdot m(t)}{R^2(t)} \quad (9)$$

$$m(t) \cdot a_T(t) = F \cdot \cos \beta(t) \cdot \cos \alpha(t) \quad (10)$$

$$m(t) \cdot a_N(t) = F \cdot \sin \beta(t) \quad (11)$$

$$a_R(t) = \dot{V}_R - \frac{V_T^2}{R} - \frac{V_N^2}{R} \quad (12)$$

$$a_T(t) = \dot{V}_T + \frac{V_R V_T}{R} - V_N \dot{I} \cos \theta - V_N \dot{\Omega} \sin I \cdot \sin \theta \quad (13)$$

$$a_N(t) = \dot{V}_N + \frac{V_R V_N}{R} + V_T \dot{I} \cos \theta + V_T \dot{\Omega} \sin I \cdot \sin \theta \quad (14)$$

$$V_R = \dot{R} \quad (15)$$

$$V_T = R(\dot{\Omega} \cos I + \dot{\theta}) \quad (16)$$

$$V_N = R(-\dot{\Omega} \cdot \sin I \cdot \cos \theta + \dot{I} \cdot \sin \theta) \quad (17)$$

$$\theta = \omega + f \quad (18)$$

The orbital transfer problem studied was formulated subjected to the dynamics in inertial coordinates, helped by the instantaneous keplerian coordinates ($\Omega, I, \omega, f, a, e$) and rewriting by the other coordinate system centered in the satellite (R,T,N) and the 9 state variables, defined and used by Biggs (1978,1979) and Prado (1989). In the centered-satellite-system we decomposed the actual thrust vector in three components, radial, transversal and normal directions.

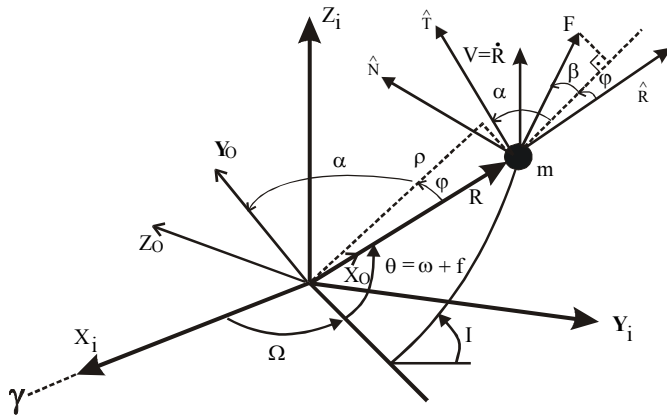


Figure 1. Reference Systems used in this work.

2. 1. The Thrust Vector Applied to the Satellite under Superposed and Correlated Deviations

The Figure (2) shows the coordinate system localized in the satellite (TRN system) and the thrust vector applied to this vehicle.

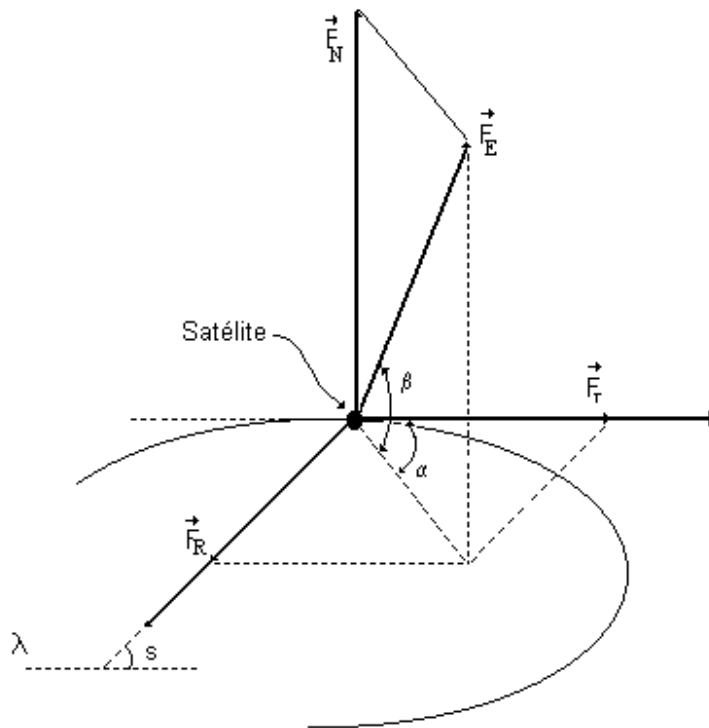


Figure 2. The Thrust Vector applied to the Satellite

The thrust components are affected by pitch and yaw during the burn. This effects can be modeled as one superposition deviations and/or correlation deviations. The thrust vector, in general, is given,

$$\vec{F}_E = \vec{F} + \Delta\vec{F} \tag{19}$$

$$\vec{F}_E = \vec{F}_R + \vec{F}_T + \vec{F}_N \tag{20}$$

$$|F_E| = F_E, \quad |F| = F \tag{21}$$

and their components to the superposition deviations case are,

$$F_R = (F + \Delta F) \cos(\beta + \Delta\beta) \sin(\alpha + \Delta\alpha) \quad (22)$$

$$F_T = (F + \Delta F) \cos(\beta + \Delta\beta) \cos(\alpha + \Delta\alpha) \quad (23)$$

$$F_N = (F + \Delta F) \sin(\beta + \Delta\beta) \quad (24)$$

with,

F , F_T and ΔF (DES1) are the vector without deviations modulus, the vector with deviations, and the vector thrust deviation, respectively; $\Delta\alpha$ (DES2) e $\Delta\beta$ (DES3) are the pitch and yaw deviations, respectively; F_R , F_T and F_N are the thrust vector components with deviations in the transversal, radial and normal directions, respectively. The DES1, DES2, DES3 are maximum deviations.

To model the correlated deviations case, we suggested one correlation function thrust deviations, given of:

$$J_n = \sum_{k=1}^{L/2} \left[k^{-z} \left(\frac{2\pi}{L} \right)^{(1-z)} \right]^{1/2} \cos \left(\frac{2\pi nk}{L} + \phi_k \right) \quad (25)$$

This function provides the individual and correlated thrust deviations ($\Delta\alpha$, $\Delta\beta$, ΔF). The approach based on the use of discrete Fourier transforms (Feder, 1992), a power-law spectral density imposed by construction whenever the deviations are given by Eq. (25). The parameter z defines as much as is strong the correlation between two consecutive deviations values. The non-correlated deviations case is obtained at $z=0$, inside the practical interest range.

3. Keplerian Elements Evolutions – Superposed Deviations

In this section we present the Monte-Carlo simulations for orbital transfers maneuvers under direction deviations in the thrust vector. We analyzed two kind of maneuvers. The first is 1) a high orbit low thrust coplanar theoretical transfer used by Biggs (1978 and 1979) and Prado (1989) to test the optimization method; 2) a middle orbit high thrust noncoplanar practical transfer (one of the transfers during the injection of the EUTELSAT II-F2 satellite) from Kuga et alli (1991). These were confirmed and improved with respect to the satisfaction of the initial and final keplerian elements. The keplerian elements we analyzed are semi-major axis (a), inclination (i), eccentricity (e), ascending node (Ω).

3.1. Semi-major Axis Evolution

The Figure (3) to (6) show the numerical cause/effect relation between final mean semi-major axis $E\{a(t_2)\}$ and the maximum deviation $\Delta\alpha_{\max} = \text{DES2} = \sqrt{J}$, $\Delta\alpha = \text{DES3} = \sqrt{J}$, $\Delta\beta = \Delta\beta_{\max}$ in the thrust angles $\alpha(t)$ and $\beta(t)$, respectively, for: a) the theoretical transfer (T); and b) the practical transfer (P). The deviations are modeled as random-bias (systematic – S) or white noise (operational - O) stochastic processes. The DES1=0,1% in Fig(3) and 5,0% in Fig (4).

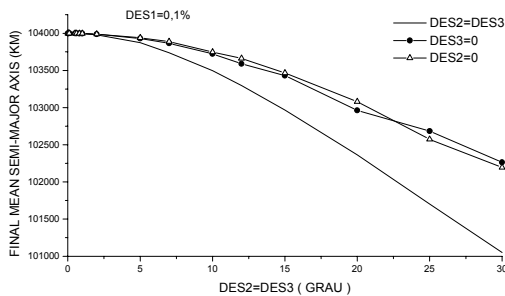


Figure 3. Mean Semi-major axis vs. DES2=DES3, TS

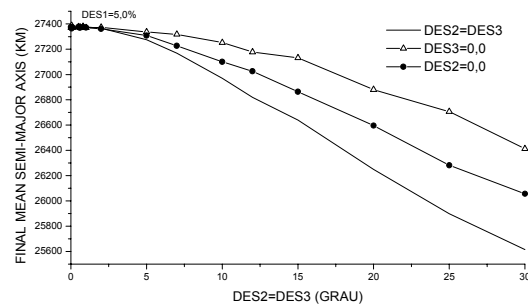


Figure 4. Mean Semi-major axis vs. DES2=DES3, PO

The first important result we found is the nonexistence of the cause/effect relation between the mean semi-major axis and DES1, that is, the modulus thrust vector deviations. Besides this, we can observe that inside practical interest range

of the direction deviations $(0,0^0$ to $2,0^0$), the behavior of the semi-major axis mean values is the same for the three cases: 1) superposed deviations; 2) non-superposed and only pitch deviations and; 3) non-superposed and only yaw deviations. The superposition effect of these deviations is evidenced only outside practical interest range. In this range the semi-major axis admits more strong decay. We observe too, that the systematic effects are more strong than operational effects for the both orbits. In the follow we show the algebraic cause/effect relation for the non-superposed $\Delta\alpha_{max}$ and the $E\{a(t_2)\}$,

$$\sum_{n=1}^{\infty} (-1)^{n+1} \frac{1}{a^{n+1}(t_2)} \cdot E\{\Delta^n a(t_2)\} = K_1 \cdot \sum_{n=1}^{\infty} (-1)^n \cdot \frac{1}{(2.n+1)!} \cdot \Delta^{2.n}\alpha_{max} \quad (26)$$

with,

$$K_1 = \frac{2}{\mu} \cdot (Q_1 + Q_2)/m \quad (27)$$

Q_1 and Q_2 are quadratures.

The Eq. (26) describes one sequence of the even power terms for the maximum deviation in "pitch" with respect the expected values of the semi-major axis. For $n=1$, we have,

$$E\{\Delta a(t_2)\} = -\frac{1}{3!} \cdot \Delta^2\alpha_{max} K_1 \cdot a^2(t_2) = -\frac{1}{3!} \cdot \Delta^2\alpha_{max} K_2 \quad (28)$$

This relation was obtained by Jesus (1999) and describes one parabolic relation for first order. The results for the different superposed deviations are showed in Fig.(5) and Fig.(6), with $DES1=5,0\%$.

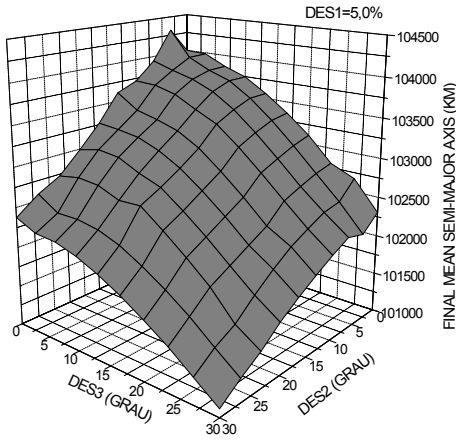


Figure 5. Mean Semi-major axis vs. $DES2 \neq DES3$, TS

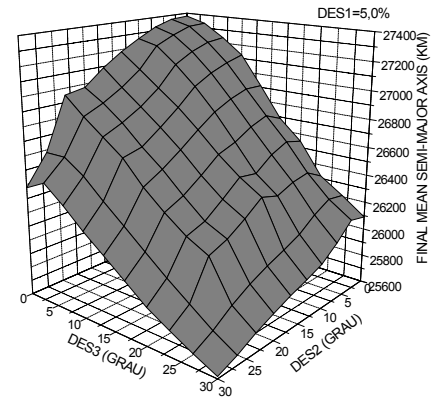


Figure 6 . Mean Semi-major axis vs. $DES2 \neq DES3$, PS

The superposition of the thrust deviations provides nonlinear relations (near the parabolic) among the mean deviations in the final semi-major axis $E\{\Delta a(t_2)\}$ to the pitch and yaw angles standard $\sigma_{\Delta\alpha}$ and $\sigma_{\Delta\beta}$ deviations for random biased and white gaussian $\Delta\alpha$ and $\Delta\beta$ in both transfers, when these deviations are equals. For the different direction deviations, the superposition provides revolution surface (near the paraboloid), which one deform outside the practical interest deviations. The Monte-Carlo simulations results showed that there is one clear cause/effect nonlinear relation between the vector thrust deviations and the final semi-major axis for the superposition case.

3.2. Inclination Evolution

The Figures (7) and (8) show the cause/effect relation between orbit inclination and the thrust deviations in the practical orbit. For the equal deviations, Fig. (7), we observed the systematic deviations affected more strongly that the operational deviations, that is, the inclinations values are more increased and the orbit deviated more to the Earth Equator. The Fig. (8) shows the results of the different direction deviations. We observed deformation surface cause/effect to $DES2$ and $DES3$ outside of the practical interest range.

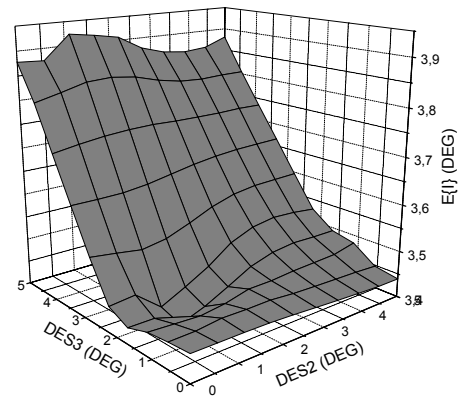
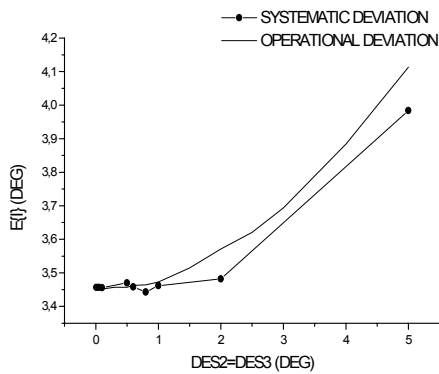


Figure 7. Final Mean Inclination vs. DES2=DES3, P

Figure 8. Final Mean Inclination vs. DES2≠DES3, P

The results to the theoretical cases did not show any dependence relation between the final mean inclination values, $E\{I(t_2)\}$, and the thrust direction deviations. It was verified small numerical fluctuations in their values.

3.3. Eccentricity Evolution

The final mean eccentricity values, $E\{e(t_2)\}$, to the theoretical orbits too did not show dependence relation with the thrust direction deviations, except outside the practical interest range, with reduction of their values. The practical case show increasing to the eccentricity values for deviations equals outside the practical interest range. The Fig. (9) and (10) show these behaviors.

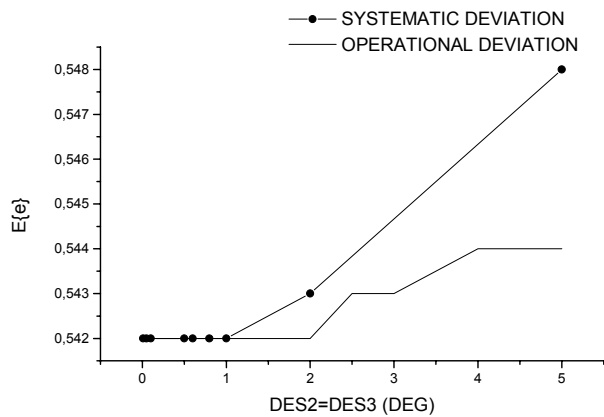
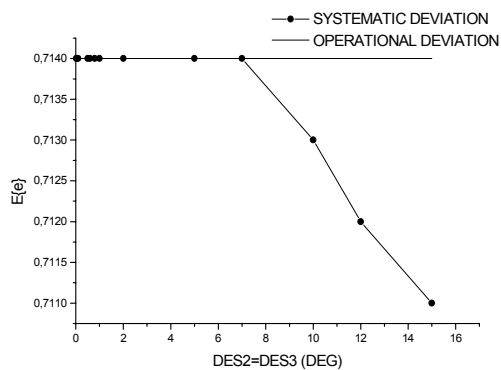


Figure 9. Final Mean Eccentricity vs. DES2=DES3, T

Figure 10. Final Mean Eccentricity vs. DES2=DES3, P

The Figures (11) and (12) show the behaviors of the practical orbit eccentricity with the different superposed direction deviations. The systematic deviations increases more the eccentricity values than the operational deviations, that is, the systematic deviations deform more the final orbit form, dilating the final ellipse, than the operational deviations. The superposition of the different deviations affect more the final eccentricity values than the superposed equal deviations.

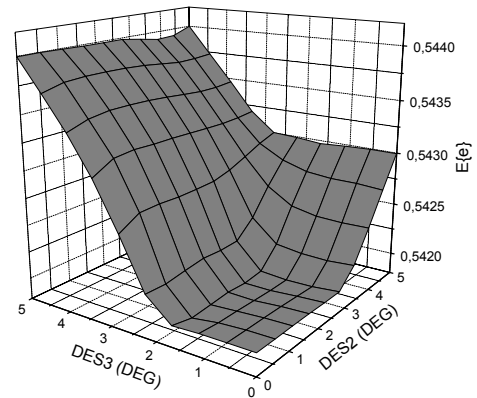
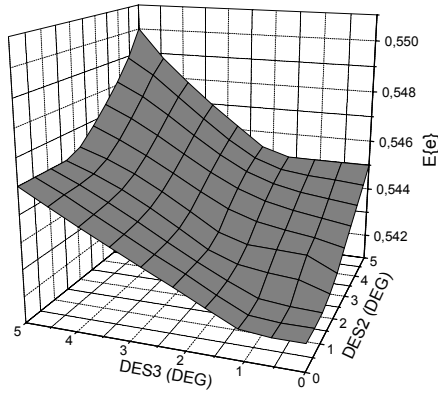


Figure 11. Final Mean Eccentricity vs. DES2≠DES3, S

Figure 12. Final Mean Eccentricity vs. DES2≠DES3, O

These results show one nonlinear relation between the final mean eccentricity values and the thrust direction deviations to the practical orbit.

3.4. Ascending Node (Ω) Evolution

The Figures (13) and (14) show the final mean ascending node values, $E\{\Omega(t_2)\}$, to different direction thrust deviation, cases operational and systematic, respectively, practical orbit. The theoretical orbit ascending node values did not modify along the burn arc under thrust direction deviations.

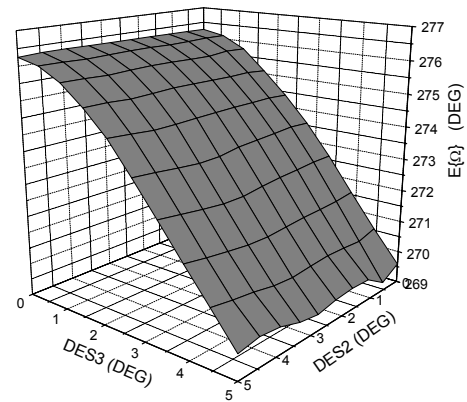
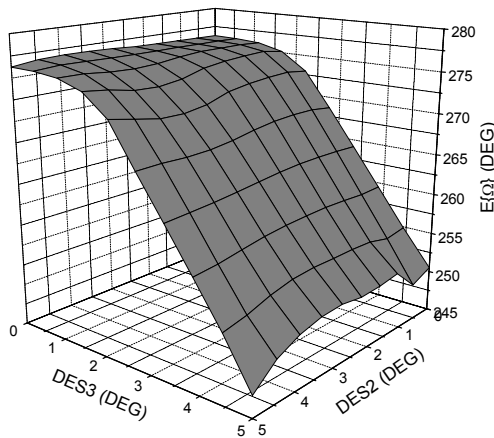


Figure 13. Final Mean Asc. Node vs. DES2≠DES3, S

Figure 14. Final Mean Asc. Node vs. DES2≠DES3, O

Clearly, we can observed the deformation of the cause/effect surfaces with the superposition of the thrust direction deviations. The final mean ascending node values are more affected through the systematic deviations. The final orbit will be more removed of the line of nodes, changing the orientation of the orbit in space.

3.5. Keplerian Elements Evolution – Correlated Deviations Case

The suggested the correlated deviations model in the Eq. (25) to study the propulsion system consuming. We expect that after the first burn, it occurs decay of the propulsion system power. So, we found one mathematical relation between the successive deviations to model the thrust deviations, that is, after many burns the accumulative deviations are products of the consuming of the propulsion system. In this section we show the results of the behaviors keplerian orbital elements through the correlated direction thrust deviations. The Fig. (15) show the semi-major axis evolution as function the correlation factor z . The practical orbit increases its final mean semi-major axis values with z . But with the superposition of the correlated deviations these values decrease strongly.

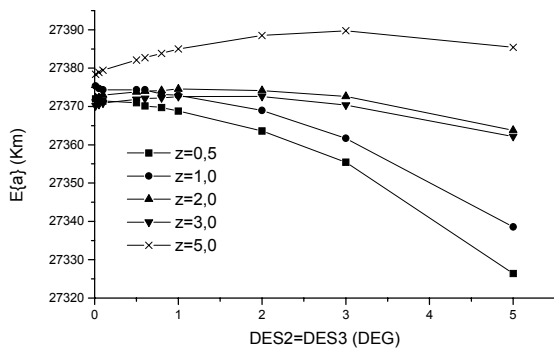


Figure 15. Final Mean Semi-major axis vs. z, P

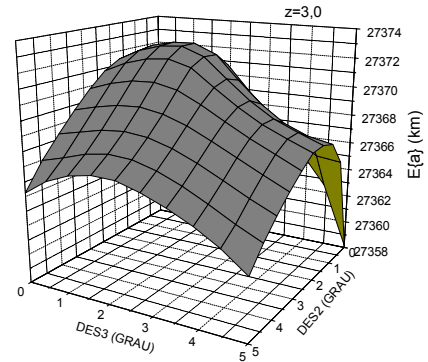


Figure 16. Final Mean Semi-major axis vs. z, P

The Fig.(16) show the cause/effect relation in the deformed paraboloid to $z=3,0$ to final mean the semi-major axis and the different superposed and correlated thrust direction deviations. We can noticed that the semi-major axis values are strongly affected through the correlation deviations w.r.t. the others cases: superposed systematic, superposed operational or individual deviations. The Fig. (17) shows the eccentricity ($z=5,0$) results and the Fig. (18) shows the inclination ($z=3,0$) results.

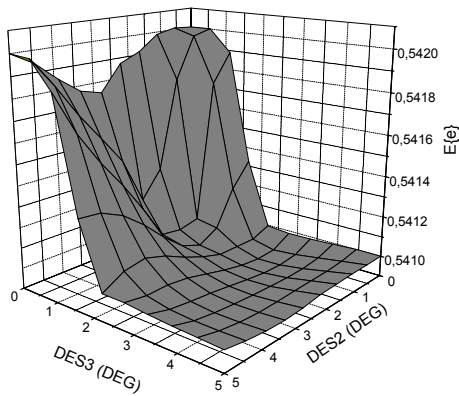


Figure 17. Final Mean Eccentricity vs. z, P

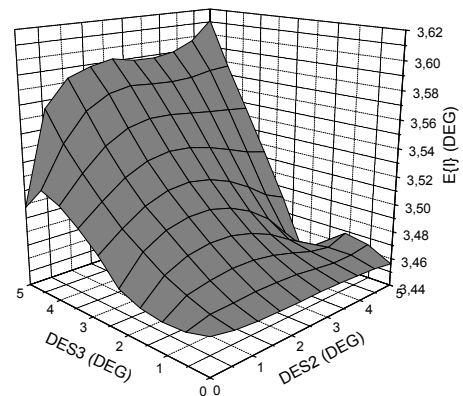


Figure 18. Final Mean Inclination vs. z, P

These figures show that the only very strong correlation affects in the eccentricity, decreasing its values. The deformation. These effect in the inclination increases its values non uniformly, because the strong dependence with the yaw angle to out-plane orbit (practical orbit). The Fig. (19) and (20) show the results of ascending node as function z.

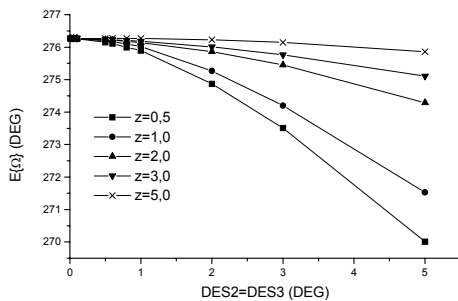


Figure 19. Final Mean Ascending Node vs. z, P

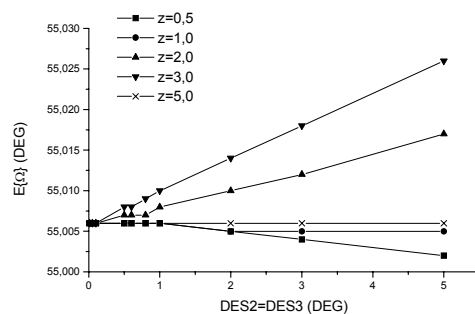


Figure 20. Final Mean Ascending Node vs. z, T

The correlation effect in the ascending node increases its final mean values in in-plane orbit (theoretical) and decreases its in out-plane orbit (practical). These results suggest that the consumed propulsion systems tends to dislocate the orbit out the reference plane, mainly, out-plane orbits.

4. The Limited Power Effects

In this section we present the numerical analysis results about the propulsion system power effects over the maneuvers. The power system can modified the thrust deviations effect through the burn arcs. We analyzed only the semi-major axis, eccentricity and inclination for the both transfers trajectories. The Fig. (21) and (22) show the final mean semi-major axis behaviors under superposition deviations and the Fig. (23) and (24) show the results about the eccentricity under systematic and operational superposed deviations, respectively.

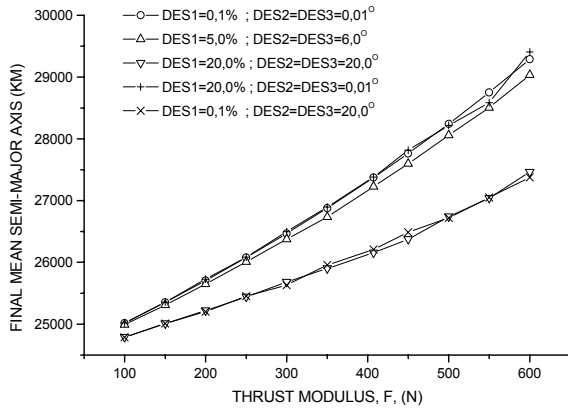


Figure 21. Final Mean Semi-major axis vs. F, PS

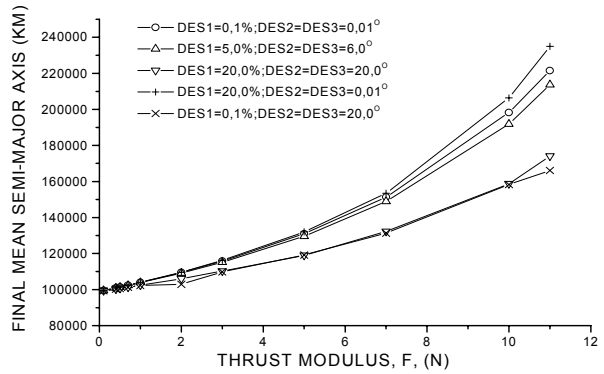


Figure 22. Final Mean Semi-major axis vs. F, TS

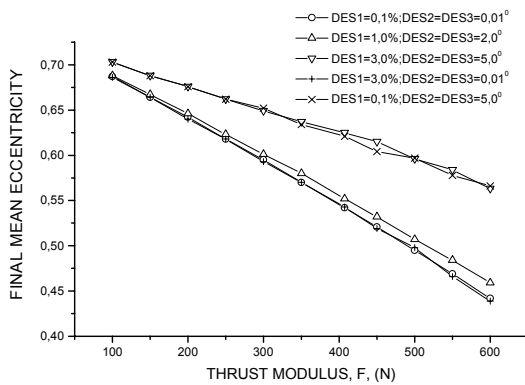


Figure 23. Final Mean Eccentricity vs. F, PS

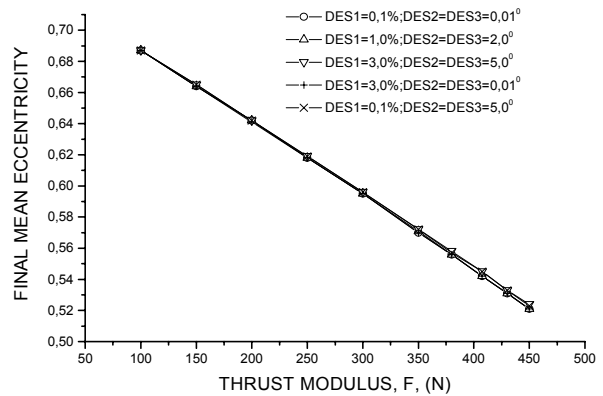


Figure 24. Final Mean Eccentricity vs. F, PO

These results show that the motor power influences the semi-major axis for the both maneuvers, increasing their values. Besides this, when the superposed direction deviations are so strong, the increasing of the motor power stabilizes their influence, minimizing their effects. Their effect over the eccentricity is to reduce their values. This decay is near linear to systematic and operational deviations. The decay is major for the systematic case. The stabilizing effect for the strong direction deviations is too verified, but, only for the systematic case. The ellipsis is more deformed in this case. The Fig. (25) and (26) show the results of the inclination for the systematic and operational deviations, respectively. The inclination behaviors under power system influence are almost different, depending of the kind of deviations (S,O). The values decay is similar to eccentricity, occurring stabilizing to more power motors under so strong operational case. To the systematic deviations case this stabilizing occurs to small and mean power motors under the same direction deviations range and to more power motors under small direction deviations with more power motors.

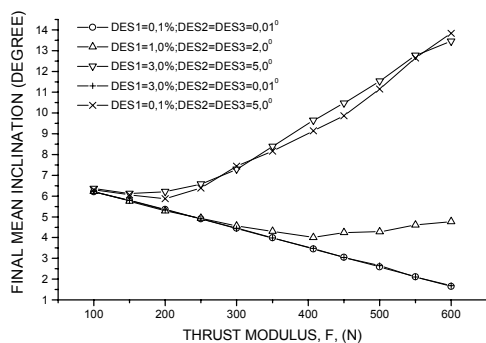


Figure 25. Final Mean Inclination vs. F, PS

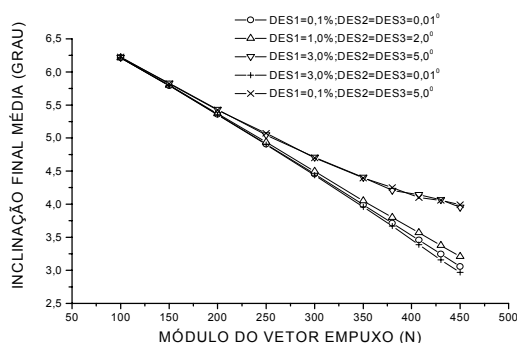


Figure 26. Final Mean Inclination vs. F, PO

5. Conclusions

In general the direction thrust deviations modify the orbit form, its inclination, dislocating it out the reference plane. There are nonlinear cause/effect relation between the keplerian orbital elements (a , e , i , Ω) studied and the thrust direction deviations. The effect of the superposition and the correlation deviations is reduce or increase the keplerian elements, modifying their final values. This fact demands more correction maneuvers and additional fuel consumption. The transfers maneuvers loss the optimality and energy because this deviations. The propulsion system power acts as stabilizer element of the direction deviations effects, recuperating the orbital damages for the so strong deviations. This approach is more close to the realistic transfer phenomenon. These propulsion variable systems can be used as orbital control system.

6. References

- Adams, N. J., Melton, R.G., 1986, "Orbit Transfer Error Analysis for Multiple, Finite Perigee Burn, Ascent Trajectories", The Journal of Astronautical Sciences, Vol. 34, No. 4, pp. 355-373.
- Biggs, M.C.B., 1978, "The Optimisation of Spacecraft Orbital Manoeuvres. Part I: Linearly Varying Thrust Angles", The Hattfield Polytechnic Numerical Optimisation Centre, Connecticut, USA.
- Biggs, M.C.B., 1979, "The Optimisation of Spacecraft Orbital Manoeuvres. Part II: Using Pontryagin's Maximum Principle", The Hattfield Polytechnic Numerical Optimisation Centre, Connecticut, USA.
- Feder, J., 1988, "Fractals", (Plenum Press., New York): A. Tsonis., 1992, "Chaos: From Theory to Applications" (Plenum Press, New York).
- Javorssek II, D. and Longuski, M. J., 1999, "Velocity Pointing Errors Associated with Spinning Thrusting Spacecraft", AIAA Paper 99-452, AIAA/AAS Astrodynamics Conference, Girdwood, Alaska, August 16-19.
- Jesus, A. D. C., Souza, M. L. O and Prado, A.F.B.A., 2002, "A Survey on the Problem of Orbital Maneuvers for an Artificial Satellite", Advances in Space Dynamics, Vol. 3, No. 1, pp. 363-396.
- Jesus, A.D.C., 1999, "Análise Estatística de Manobras Orbitais com Propulsão Finita Sujeita a Erros no Vetor Empuxo". Doctoral Thesis. INPE, São José dos Campos, São Paulo, Brazil.
- Kluever, C.A. and Tanck, G.S., 1997, "A Feedback Control Law for Stationkeeping with on-off Thrusters", Advances in the Astronautical Sciences, Vol. 97, No. 3, pp. 387-399.
- Kuga, H.K., Gill, E. and Montenbruck, O., 1991, "Orbit Determination and Apogee Boost Maneuver Estimation Using UD Filtering". Internal Report DLR-GSOC IB 91-2. Wesling, Germany.
- Maciejewski, A., 1995, "Reduction, Relative Equilibria and Potential in the two Rigid Bodies Problem", Celestial Mechanics and Dynamical Astronomy, Vol. 63, pp. 1-28.
- Prado, A.F.B.A., 1989, "Análise, Seleção e Implementação de Procedimentos que Visem Manobras Ótimas de Satélites Artificiais". Dissertação de Mestrado. INPE, São José dos Campos, São Paulo, Brazil.
- Porcelli, G., Vogel, E., 1980, "Two-Impulse Orbit Transfer Error Analysis Via Covariance Matrix". Journal of Spacecraft and Rockets, Vol. 17, No. 3, pp. 248-255.
- Rodrigues, D.L.F., 1991, "Análise Dinâmica da Transferência Orbital". Master Dissertation. INPE, São José dos Campos, São Paulo, Brazil.
- Santos-Paulo, M.M.N., 1998, "Estudo de Manobras Tridimensionais Impulsivas pelo Método de Altman e Pistiner, com Erros nos Propulsores". Master Dissertation. INPE, São José dos Campos, São Paulo, Brazil.
- Ulybyshev, Y., 1998, "Long Term Formation Keeping of Satellite Constellation Using Linear-Quadratic Controller", Journal of Guidance, Control and Dynamics, Vol. 21, No. 1, pp. 109-115.
- Vassar, R. H. and Sherwood, R.B., 1985, "Formationkeeping for a Pair of Satellites in a Circular Orbit", Journal of Guidance, Control and Dynamics, Vol. 8, No. 2, pp. 235-242.

